PROCEEDINGS OF SCIENCE

Quark mass dependence of the nuclear LS force

Takuya Sugiura[a,b,*]

[a] *Faculty of Data Science, Rissho University, Kumagaya, 360-0194, Japan*
[b] *Interdisciplinary Theoretical and Mathematical Sciences Program (iTHEMS), RIKEN, Wako, 351-0198, Japan*

E-mail: sugiura@rcnp.osaka-u.ac.jp

We study the quark-mass dependence of the nuclear spin-orbit (LS) force in lattice QCD using the HAL QCD method with the free Laplacian Heaviside (fLapH) source operator. From flavor-SU(3) symmetric gauge ensembles at $m_{\rm PS} \simeq 837$, 672, and 469 MeV, we extract the central, tensor, and LS forces in the $(S, I) = (1, 1)$ sector. The central force is found to be repulsive and the LS force attractive, with both becoming stronger toward lighter quark masses. These contributions largely cancel in the $^3P_2$ channel, resulting in a repulsive potential with only mild quark-mass dependence. These results do not support the emergence of $^3P_2$ neutron superfluidity at the quark masses considered here.

The 42nd International Symposium on Lattice Field Theory (LATTICE2025)
2-8 November 2025
Tata Institute of Fundamental Research, Mumbai, India

*Speaker

https://pos.sissa.it/

PoS(LATTICE2025)060

1. Introduction

The nuclear force plays a central role in understanding the properties of atomic nuclei and nuclear matter. Over the past decades, a variety of theoretical approaches have been developed to study nuclear systems based on nucleon-nucleon interactions, including *ab initio* calculations of light nuclei, shell-model studies of medium-mass nuclei, and many-body methods applied to nuclear matter [1]. In particular, not only the central and tensor forces but also the spin-orbit (LS) force is indispensable for a quantitative understanding of nuclear structure and dense matter.

Among the spin-triplet odd-parity channels, the $^3P_2$ channel is of special interest because it is closely related to neutron superfluidity in dense neutron matter. Phenomenological nucleon-nucleon interactions generally exhibit an attractive pocket in this channel [2], which is considered important for the onset of $^3P_2$ pairing. It is therefore an important problem to clarify how such a feature emerges directly from QCD.

The HAL QCD method provides a framework to extract hadron-hadron interactions from lattice QCD through the Nambu-Bethe-Salpeter wave function and its associated non-local potential. In previous lattice studies, the central, tensor, and LS forces in the odd-parity sector have been investigated, and the existence of a weak attractive pocket in the $^3P_2$ channel has been suggested [3]. On the other hand, a systematic understanding of the quark-mass dependence of the nuclear LS force and of the resulting P-wave interactions is still limited.

In this work, we investigate the quark-mass dependence of the nuclear LS force in lattice QCD by employing the HAL QCD method together with the free Laplacian Heaviside (fLapH) source operator. The fLapH setup enables an efficient treatment of two-nucleon systems with non-zero relative momentum and is therefore suitable for odd-parity channels.

2. Determination of the NN potential

The Nambu-Bethe-Salpeter (NBS) wave function is defined as

$$\psi_{\alpha\beta}(\boldsymbol{x}-\boldsymbol{y};W) \equiv \langle 0|p_\alpha(\boldsymbol{x})n_\beta(\boldsymbol{y})|W\rangle, \tag{1}$$

where $p_\alpha(\boldsymbol{x})$ and $n_\beta(\boldsymbol{y})$ denote local interpolating operators for proton and neutron, respectively, and $|W\rangle$ are the QCD energy eigenstates with the same quantum numbers as the NN system and the total energy $W = 2\sqrt{k^2+m_N^2}$. Below the inelastic threshold of the NN system $W < 2m_N + m_\pi$, a non-local and energy-independent potential can be defined through [4, 5]

$$\left(\frac{k^2}{m_N} - H_0\right)\psi(\boldsymbol{r};W) = \int d^3\boldsymbol{r}U(\boldsymbol{r},\boldsymbol{r}')\psi(\boldsymbol{r}';W) \tag{2}$$

with the nucleon mass m_N and $H_0 \equiv -\boldsymbol{\nabla}^2/m_N$. The non-local potential satisfying Eq. (2) for all energies below the threshold is not uniquely determined. We introduce the derivative expansion up to the next-to-leading order

$$U(\boldsymbol{r},\boldsymbol{r}') = \left[V_c^I(r) + V_t^I(r)S_{12} + V_{ls}^I(r)\boldsymbol{L}\cdot\boldsymbol{S} + O(\boldsymbol{\nabla}_r^2)\right]\delta^3(\boldsymbol{r}-\boldsymbol{r}'), \tag{3}$$

where $S_{12} \equiv 3(\boldsymbol{\sigma}_1\cdot\hat{\boldsymbol{r}})(\boldsymbol{\sigma}_2\cdot\hat{\boldsymbol{r}}) - \boldsymbol{\sigma}_1\cdot\boldsymbol{\sigma}_2$, $\boldsymbol{L} \equiv -i\boldsymbol{r}\times\boldsymbol{\nabla}$, $\boldsymbol{S} = (\boldsymbol{\sigma}_1+\boldsymbol{\sigma}_2)/2$, and $I = 0, 1$ denote the total isospin.

PoS(LATTICE2025)060

In actual lattice QCD calculations, one computes the nucleon correlation function

$$R^{(\Gamma)}_{\alpha\beta}(\boldsymbol{r},t) \equiv \frac{1}{V}\sum_{\boldsymbol{x}}\langle 0|T p_\alpha(\boldsymbol{r}+\boldsymbol{x},t) n_\beta(\boldsymbol{x},t)\bar{\mathcal{J}}^{(\Gamma)}|0\rangle / e^{-2m_N t} \tag{4}$$

$$= \sum_n \psi_{\alpha\beta}(\boldsymbol{r};W_n)\langle W_n|\bar{\mathcal{J}}^{(\Gamma)}|0\rangle e^{-\Delta W_n t}, \tag{5}$$

where $\Delta W_n \equiv W_n - 2m_N$ and the source operator $\bar{\mathcal{J}}^{(\Gamma)}$ couples to the two-nucleon states with $\Gamma = (J^\Pi, J_z, S)$. The explicit construction of the source operator is described in Sect. 3. When t is large enough such that the contribution from the inelastic states is negligible, one can show that the non-local potential in Eq. (2) satisfies the following time-dependent equation [3, 6]:

$$\left\{\frac{1}{c^2_{\text{eff}}}\left(\frac{1}{4m_N}\frac{\partial^2}{\partial t^2} - \frac{\partial}{\partial t}\right) - H_0\right\} R^{(\Gamma)}(\boldsymbol{r},t) = \int d^3\boldsymbol{r}' U(\boldsymbol{r},\boldsymbol{r}') R^{(\Gamma)}(\boldsymbol{r}',t). \tag{6}$$

The factor $c^2_{\text{eff}} \equiv \frac{E(p)^2 - E(0)^2}{p^2}$ represents a violation of the relativistic dispersion relation.

We define an inner product of the correlation functions as $\langle F(\boldsymbol{r})G(\boldsymbol{r})\rangle \equiv \sum_{g\in O_h} F^*_{\alpha\beta}(g\boldsymbol{r})G_{\alpha\beta}(g\boldsymbol{r})$ to reduce unphysical statistical noise. Since the local potentials $V^I_c(r)$, $V^I_t(r)$, and $V^I_{ls}(r)$ in Eq. (3) are invariant under the cubic group rotations, they can be determined in the $I = 1$ sector by solving the following equation:

$$V^{I=1}_c(r)F^{(\Gamma)}_c(r) + V^{I=1}_t(r)F^{(\Gamma)}_t(r) + V^{I=1}_{ls}(r)F^{(\Gamma)}_{ls}(r) = K^{(\Gamma)}(r), \tag{7}$$

where

$$F^{(\Gamma)}_c(r) \equiv \langle R^{(\Gamma)}(\boldsymbol{r},t), R^{(\Gamma)}(\boldsymbol{r},t)\rangle \tag{8}$$

$$F^{(\Gamma)}_t(r) \equiv \langle R^{(\Gamma)}(\boldsymbol{r},t), S_{12}R^{(\Gamma)}(\boldsymbol{r},t)\rangle \tag{9}$$

$$F^{(\Gamma)}_{ls}(r) \equiv \langle R^{(\Gamma)}(\boldsymbol{r},t), (\boldsymbol{L}\cdot\boldsymbol{S})R^{(\Gamma)}(\boldsymbol{r},t)\rangle \tag{10}$$

$$K^{(\Gamma)}(r) \equiv \langle R^{(\Gamma)}(\boldsymbol{r},t), (D_t - H_0)R^{(\Gamma)}(\boldsymbol{r},t)\rangle \tag{11}$$

and $D_t \equiv \left(\frac{1}{4m_N}\frac{\partial^2}{\partial t^2} - \frac{\partial}{\partial t}\right)/c^2_{\text{eff}}$. In order to obtain three unknown functions $V^I_c(r)$, $V^I_t(r)$, and $V^I_{ls}(r)$, we employ $J^\Pi = A^-_1, T^-_1, E^-$ in Eq. (7), corresponding to the ${}^3P_0$, ${}^3P_1$, and ${}^3P_2$ states in the continuum, respectively. Another choice of representations, $J^\Pi = A^-_1, T^-_1, T^-_2$, does not lead to a significant difference.

3. Source Operator

In order to access the P-wave states, the source operator must couple to two-nucleon states with non-zero relative momentum $\boldsymbol{q}$. This naively requires all-to-all propagators and is computationally demanding. An alternative approach has been proposed in Ref. [7]. The method known as Laplacian Heaviside (LapH), here referred to as covariant LapH (cLapH), provides a low-rank approximation to all-to-all propagators by projecting quark fields onto a low-dimensional subspace spanned by low eigenmodes of the gauge-covariant Laplacian. It has been extended to stochastic estimation [8] and has been successfully applied to hadron spectroscopy and scattering studies [9–13]. We employ an approach that is similar to cLapH but computationally more efficient in the HAL QCD framework and refer to it as free LapH (fLapH) [14].

The fLapH distillation operator is defined as

$$\mathcal{S}(\boldsymbol{x}, \boldsymbol{y}) \equiv \frac{1}{N_v} \sum_{l=1}^{N_v} v_l(\boldsymbol{x}) v_l^*(\boldsymbol{y}), \tag{12}$$

where $v_l(\boldsymbol{x}) = \exp(i\boldsymbol{p}_l \cdot \boldsymbol{x})$ denotes a plane wave with momentum $\boldsymbol{p}_l = 2\pi L^{-1}\boldsymbol{n}_l$, and the index l labels the modes in ascending order of $|\boldsymbol{n}_l|$, with $\boldsymbol{n}_l \in \mathbb{Z}^3$. This is a projection onto a subspace spanned by the N_v lowest-lying eigenmodes of the free Laplacian, equivalent to imposing a momentum cutoff on the quark fields. Since we are interested in low-energy nucleon scattering, high eigenmodes are expected to be irrelevant, so that N_v can be taken much smaller than the lattice volume $V = L^3$ required for the all-to-all propagators. We also note that $N_v = 1$ is equivalent to the conventional wall source operator.

The fLapH-distilled nucleon creation operators read

$$\bar{N}(\boldsymbol{q}, t_0) = \frac{1}{V} \sum_{\boldsymbol{x}} e^{i\boldsymbol{q}\cdot\boldsymbol{x}} \epsilon_{abc} \left(\bar{q}^a_{f_1}\mathcal{S}\right)(\boldsymbol{x}, t_0) \left[\left(\bar{q}^b_{f_2}\mathcal{S}\right)(\boldsymbol{x}, t_0)^T C\gamma_5 \left(\bar{q}^c_{f_3}\mathcal{S}\right)(\boldsymbol{x}, t_0)\right] \tag{13}$$

$$= \sum_{l_1,l_2,l_3} \delta_{\boldsymbol{q},\boldsymbol{p}_{l_1}+\boldsymbol{p}_{l_2}+\boldsymbol{p}_{l_3}} \epsilon_{abc} \bar{q}^a_{f_1,l_1}(t_0) \left[\bar{q}^b_{f_2,l_2}(t_0)^T C\gamma_5 \bar{q}^c_{f_3,l_3}(t_0)\right], \tag{14}$$

$$\bar{q}^a_{f,l}(t_0) \equiv \frac{1}{N_v} \sum_{\boldsymbol{x}} \bar{q}^a_f(\boldsymbol{x}, t_0) v_l(\boldsymbol{x}). \tag{15}$$

Then the two-nucleon source operator with relative momentum $\boldsymbol{q}$ and zero total momentum reads

$$\bar{J}(\boldsymbol{q}, t_0) = \bar{p}(+\boldsymbol{q}, t_0)\bar{n}(-\boldsymbol{q}, t_0). \tag{16}$$

Following Ref. [3], projection matrices onto irreducible representations are constructed. We fix $q \equiv |\boldsymbol{q}| = 2\pi n L^{-1}$ and take $\boldsymbol{q}$ to be one of the on-axis momenta, $\boldsymbol{q}_1 = (q, 0, 0), \boldsymbol{q}_2 = (0, q, 0), \boldsymbol{q}_3 = (0, 0, q), \boldsymbol{q}_4 = (-q, 0, 0), \boldsymbol{q}_5 = (0, -q, 0), \boldsymbol{q}_6 = (0, 0, -q)$. Under a cubic group rotation $g \in O_h$, Eq. (16) transforms as

$$J_{\alpha\beta}(\boldsymbol{q}_i, t_0) \mapsto \bar{p}_{\alpha'}(g^{-1}\boldsymbol{q}_i, t_0)\bar{n}_{\beta'}(-g^{-1}\boldsymbol{q}_i, t_0) S_{\alpha'\alpha}(g^{-1}) S_{\beta'\beta}(g^{-1}) \tag{17}$$

$$= J_{\alpha'\beta'}(\boldsymbol{q}_j, t_0) U_{ji}(g) S_{\alpha'\alpha}(g^{-1}) S_{\beta'\beta}(g^{-1}), \tag{18}$$

where $S(g)$ and $U(g)$ denote rotation matrices in spinor and coordinate space, respectively. Using this property, projection matrices for the total angular momentum $P^{(J)}$, $P^{(J_z)}$, parity $P^{(\Pi)}$, and the total spin $P^{(S)}$ are defined. The eigenvectors $\eta^{(J,J_z,\Pi,S);\xi}_{\alpha\beta i}$ are obtained by solving

$$\left(P^{(J)} P^{(J_z)} P^{(\Pi)} P^{(S)}\right)_{\alpha\beta i;\alpha'\beta' j} \eta^{(J^\Pi,J_z,S);\xi}_{\alpha'\beta' j} = \eta^{(J^\Pi,J_z,S);\xi}_{\alpha\beta i} \tag{19}$$

for physically allowed combinations. An additional index ξ is introduced to account for possible degeneracies, while we find that varying ξ has negligible effects on the results as long as J, J_z, Π, S are fixed. Finally, the projected two-nucleon source operator is given by

$$\bar{\mathcal{J}}^{(J^\Pi,J_z,S)} \equiv \sum_{\alpha\beta i} J_{\alpha\beta}(\boldsymbol{q}_i, t_0) \eta^{(J^\Pi,J_z,S);\xi*}_{\alpha\beta i}. \tag{20}$$

The diluted quark propagators $y_l \equiv \sum_{\boldsymbol{y}} \langle q(\boldsymbol{x}, t)\bar{q}(\boldsymbol{y}, t_0)v_l(\boldsymbol{y})\rangle$ are obtained by solving $Dy_l = v_l$, where D is the Dirac matrix. The correlation function in Eq. (4) is evaluated by the block algorithm [15]: the color, spinor, and the level contractions in the sink are performed as greedily as possible to construct proton and neutron blocks; then the other indices are contracted. Here lies a key advantage of fLapH over cLapH: while the computational cost of FFT for diagrams involving quark exchange scales as $O\left((N_c N_v)^4\right)$ in cLapH [1], it is reduced to $O(N_c^2 N_v^3)$ in fLapH thanks to the exact momentum conservation relation in Eq. (14). In our setup, this corresponds to an approximate 109-fold speed-up.

4. Lattice Setup

We use the $N_f = 3$ gauge ensembles in the flavor-SU(3) limit generated in Ref. [16]. These configurations were produced with the renormalization-group improved Iwasaki gauge action and the nonperturbatively $O(a)$-improved Wilson quark action at $\beta = 1.83$, corresponding to a lattice spacing $a = 0.121(2)$ fm. In this work, we employ the 32^4 ensembles, which give a spatial extent $L \simeq 3.87$ fm, and select the three ensembles with the common hopping parameter $\kappa_{uds} = 0.13760$, 0.13800, and 0.13840. The corresponding pseudoscalar masses are $m_{\text{PS}} \simeq 837$, 672, and 469 MeV, respectively.

The number of fLapH modes is taken to be $N_v = 19$, corresponding to the number of momentum modes $\boldsymbol{p}_l = 2\pi L^{-1}\boldsymbol{n}_l$ with $|\boldsymbol{n}_l|^2 \leq 2$, and hence to a momentum cutoff $\sqrt{2}(2\pi L^{-1}) = 604$ MeV. We take the average over the source time slices $t = 0, 2, \ldots, 30$, at which the Coulomb gauge fixing is applied. The relative momentum between the source nucleons is taken to be $|\boldsymbol{q}| = 2\pi L^{-1}$.

5. Results and Discussion

The nucleon mass and the factor c_{eff}^2 in Eq. (6) are estimated from the point-sink-fLapH-source nucleon two-point correlation functions. The results are summarized in Table 1. In addition, the exponential factor in Eq. (4) is replaced by the nucleon two-point functions to possibly cancel the elastic-state contamination.

Figure 1 shows the potentials in the $(S, I) = (1, 1)$ sector and their quark-mass dependence. We observe that the central potential is positive and the LS force is negative at all distances, and the tensor force is positive and weak. These observations are consistent with phenomenological

[1] Since the cLapH subspace is spanned by vectors carrying both spatial and color degrees of freedom, the effective number of modes is N_c times larger than that of fLapH.

Table 1: The pseudoscalar and nucleon masses, and the c_{eff}^2 factor for each gauge ensemble. The numbers in parentheses denote the statistical uncertainties estimated by the jackknife method, while the pseudoscalar masses are taken from Ref. [16].

κ_{uds}	m_{PS} [MeV]	m_N [MeV]	c_{eff}^2
0.13760	836.5(5)	1753.1(2.3)	0.955(5)
0.13800	672.3(6)	1492.5(1.8)	0.944(9)
0.13840	468.6(7)	1165.5(4.2)	0.928(6)

potentials [2] and previous lattice QCD calculations [3]. As the quark mass decreases, the absolute value of each term increases: the central force becomes more positive and the LS force more negative. Here and in what follows, the sink time slice $t = 10a$ is used. We have confirmed that varying t by a few lattice units leads to statistically consistent results.

Figure 2 shows the potentials in the $^3P_0$, $^3P_1$, and $^3P_2$ channels:

$$V^{(^3P_0)}(r) = V_c^{I=1}(r) - 4V_t^{I=1}(r) - 2V_{ls}^{I=1}(r) \tag{21}$$

$$V^{(^3P_1)}(r) = V_c^{I=1}(r) + 2V_t^{I=1}(r) - V_{ls}^{I=1}(r) \tag{22}$$

$$V^{(^3P_2)}(r) = V_c^{I=1}(r) - \frac{2}{5}V_t^{I=1}(r) + V_{ls}^{I=1}(r) \tag{23}$$

for the $m_{PS} \simeq 470\,\text{MeV}$ ensemble. We observe that these potentials are repulsive at all distances. The absence of an attractive pocket in the $^3P_2$ channel contradicts phenomenological predictions, leading to a result that cannot account for $^3P_2$ neutron superfluidity. The quark-mass dependence in the $^3P_2$ channel is found to be rather mild. This can be understood from Eq. (23): although the central and LS terms enter with the same sign, the central force is positive whereas the LS force is negative. As the quark mass decreases, both contributions increase in magnitude but in opposite directions, leading to a substantial cancellation in the overall $^3P_2$ interaction. Possible reasons for this are as follows: (1) The quark masses are not physical: even in the lightest case, $m_{PS} \simeq 470\,\text{MeV}$, and the calculations are carried out in the flavor-SU(3) limit. (2) The number of fLapH modes, $N_v = 19$, may not be sufficiently large, and the source operator has only a poor overlap with the elastic states. However, neither of these issues appears to provide a fully satisfactory explanation, given that Ref. [3] reported a weak attractive pocket in the $^3P_2$ channel despite using much heavier quark masses, $m_{PS} \simeq 1133\,\text{MeV}$ and $m_N \simeq 2158\,\text{MeV}$, as well as less sophisticated momentum-wall source operators. To clarify this point, calculations using more realistic lattice QCD configurations, such as the physical-point ensembles of Ref. [17], will be necessary in the future.

The scattering phase shifts are then calculated as follows. We fit the central and LS forces using a three-Gaussian form $v(r) = \sum_{i=1}^{3} b_i \exp\left[-\nu_i (r/a)^2\right]$, and the tensor force using a phenomenological function $v(r) = c_1(r/a)\exp\left[-\nu_1(r/a)^2\right] + c_2(r/a)^3\exp\left[-\nu_2(r/a)^2\right]$, where $a = 0.121$ fm is the lattice spacing. The potentials exhibit singular behavior at long distances due to large condition numbers in solving Eq. (7). Such behavior should simply be regarded as unphysical noise. We therefore restrict the fitting range to $r < 1.5$ fm, which is short enough to avoid the singular behavior and yet long enough to accommodate the interaction range. The fitted potentials are then used to solve the Lippmann-Schwinger equation and to extract the asymptotic behavior of the regular solutions. The scattering phase shifts and the mixing angle at $m_{PS} \simeq 470\,\text{MeV}$ in the $^3P_2 - {}^3F_2$ coupled channels are shown in Fig. 3. We see that the interaction is very weak at low energies, consistent with the absence of an attractive pocket in the $^3P_2$ channel, as already discussed above.

6. Conclusion

We have investigated the quark-mass dependence of the nuclear LS force in lattice QCD using the HAL QCD method with the fLapH source operator. From flavor-SU(3) symmetric gauge ensembles at $m_{\text{PS}} \simeq 837$, 672, and 469 MeV, we extracted the central, tensor, and LS forces in the

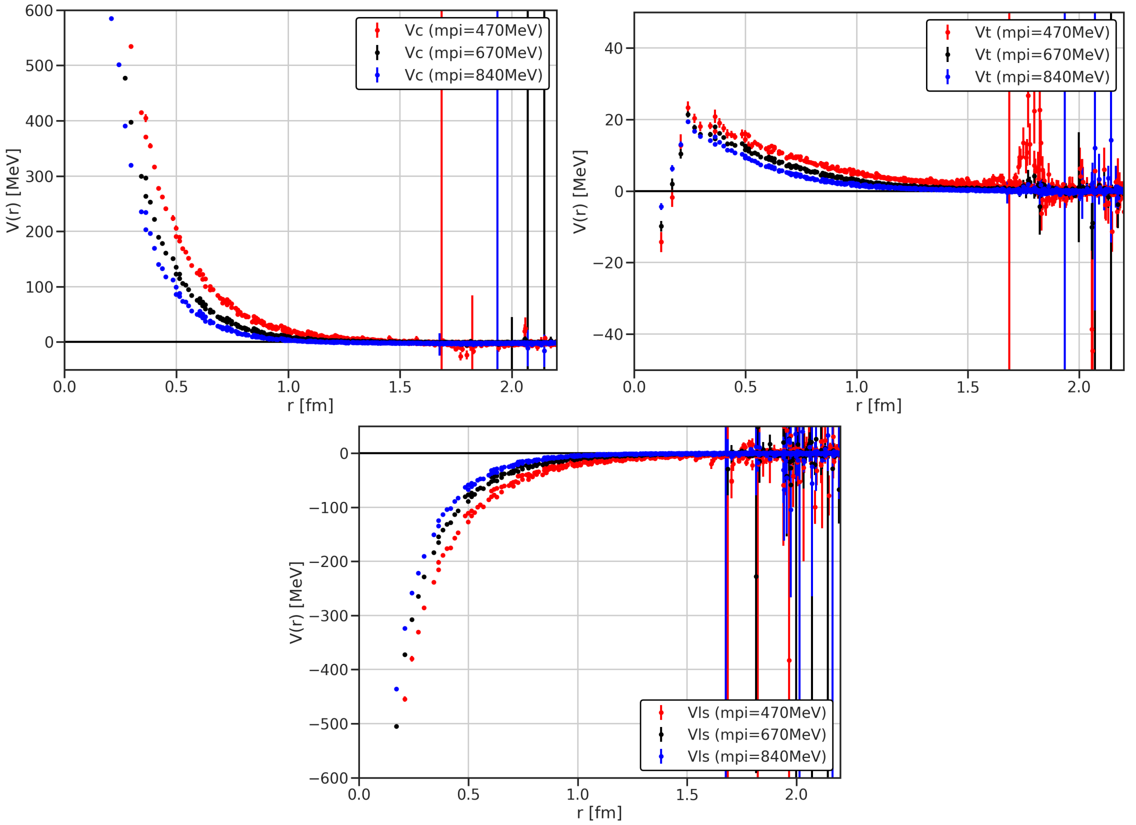

Figure 1: (Top left) Central, (top right) tensor and (bottom) LS forces in the $(S, I) = (1, 1)$ sector. The quark-mass dependence is indicated by color: (red) $m_{\mathrm{PS}} \simeq 470$ MeV, (black) 670 MeV, and (blue) 840 MeV.

$(S, I) = (1, 1)$ sector. We found that the central force is positive and the LS force is negative over the entire range, while their magnitudes become larger toward lighter quark masses.

We found that the potentials in the $^3P_0$, $^3P_1$, $^3P_2$ channels are all repulsive at all distances. No attractive pocket was observed in $^3P_2$. We also found that the quark-mass dependence in the $^3P_2$ channel is rather mild. This can be understood from the fact that the central and LS forces contribute in opposite directions to the $^3P_2$ interaction, so that their quark-mass dependences largely cancel each other.

A more definitive understanding of the odd-parity nuclear force, especially in the $^3P_2$ channel, will require calculations on more realistic gauge configurations closer to the physical point. Such studies will be essential for clarifying the QCD origin of the spin-orbit force and its role in P-wave neutron pairing.

Acknowledgements

We thank the members of the HAL QCD Collaboration for fruitful discussion and suggestions. The lattice QCD calculations have been performed on supercomputer Fugaku at RIKEN. We have used Bridge++ code [18, 19] to compute the diluted quark propagators. This work is partially supported by HPCI System Research Project (hp120281, hp200095, hp200130, hp210165, hp210117,

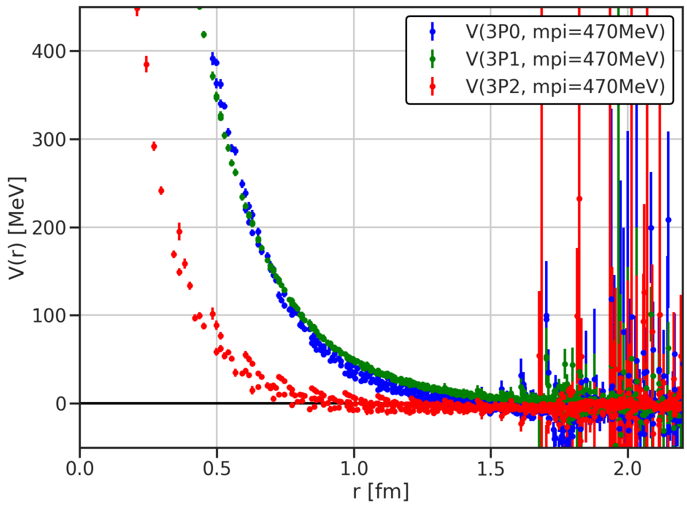

Figure 2: Potentials in the ${}^3P_0$, ${}^3P_1$, and ${}^3P_2$ channels at $m_{PS} \simeq 470$ MeV.

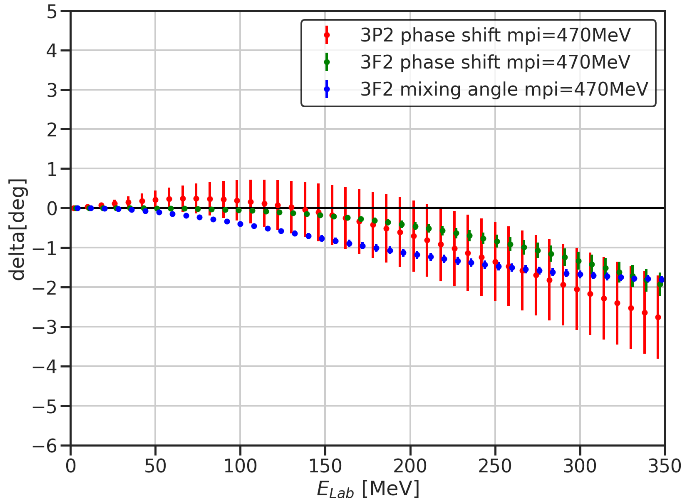

Figure 3: The scattering phase shifts and the mixing angle in the ${}^3P_2 - {}^3F_2$ coupled channels.

hp220066, hp220096, hp220174, hp230207, hp230075, hp240157, hp240213, hp250195, hp250224), JSPS Grant (JP18H05236, JP16H03978, JP19K03879, JP18H05407, JP22H00129, JP22H04917, JP23H05439, JP24K17049, JP25K17384), MOST-RIKEN Joint Project “Ab initio investigation in nuclear physics”, “Priority Issue on Post-K computer” (Elucidation of the Fundamental Laws and Evolution of the Universe), “Program for Promoting Researches on the Supercomputer Fugaku” (Simulation for basic science: from fundamental laws of particles to creation of nuclei) and (Simulation for basic science: approaching the new quantum era) (Grants No. JPMXP1020200105, JPMXP1020230411), and Joint Institute for Computational Fundamental Science (JICFuS).

References

[1] H. Hergert, *A Guided Tour of ab initio Nuclear Many-Body Theory*, *Front. in Phys.* **8** (2020) 379 [nucl-th/2008.05061].

[2] R.B. Wiringa, V.G.J. Stoks and R. Schiavilla, *An Accurate nucleon-nucleon potential with charge independence breaking*, *Phys. Rev. C* **51** (1995) 38 [/nucl-th/9408016].

[3] HAL QCD collaboration, *Spin–orbit force from lattice QCD*, *Phys. Lett. B* **735** (2014) 19 [hep-lat/1305.2293].

[4] N. Ishii, S. Aoki and T. Hatsuda, *The Nuclear Force from Lattice QCD*, *Phys. Rev. Lett.* **99** (2007) 022001 [nucl-th/0611096].

[5] S. Aoki, T. Hatsuda and N. Ishii, *Theoretical Foundation of the Nuclear Force in QCD and its applications to Central and Tensor Forces in Quenched Lattice QCD Simulations*, *Prog. Theor. Phys.* **123** (2010) 89 [hep-lat/0909.5585].

[6] HAL QCD collaboration, *Hadron–hadron interactions from imaginary-time Nambu–Bethe–Salpeter wave function on the lattice*, *Phys. Lett. B* **712** (2012) 437 [hep-lat/1203.3642].

[7] Hadron Spectrum collaboration, *A Novel quark-field creation operator construction for hadronic physics in lattice QCD*, *Phys. Rev. D* **80** (2009) 054506 [hep-lat/0905.2160].

[8] C. Morningstar, J. Bulava, J. Foley, K.J. Juge, D. Lenkner, M. Peardon et al., *Improved stochastic estimation of quark propagation with Laplacian Heaviside smearing in lattice QCD*, *Phys. Rev. D* **83** (2011) 114505 [hep-lat/1104.3870].

[9] Hadron Spectrum collaboration, *Flavor structure of the excited baryon spectra from lattice QCD*, *Phys. Rev. D* **87** (2013) 054506 [hep-ph/1212.5236].

[10] Hadron Spectrum collaboration, *Excited and exotic charmonium spectroscopy from lattice QCD*, *JHEP* **07** (2012) 126 [hep-ph/1204.5425].

[11] Baryon Scattering (BaSc) collaboration, *Nucleon-nucleon scattering from distillation*, *PoS* **LATTICE2022** (2023) 200 [hep-lat/2212.09587].

[12] Hadron Spectrum collaboration, *Quark mass dependence of $\pi\pi$ scattering in isospin 0, 1, and 2 from lattice QCD*, *Phys. Rev. D* **108** (2023) 034513 [hep-lat/2303.10701].

[13] Baryon Scattering (BaSc) collaboration, *Two-Pole Nature of the Λ(1405) resonance from Lattice QCD*, *Phys. Rev. Lett.* **132** (2024) 051901 [hep-lat/2307.10413].

[14] T. Sugiura, Y. Akahoshi, T. Aoyama, T.M. Doi and T. Doi, *Nuclear force with LapH smearing*, *PoS* **LATTICE2021** (2022) 565 [hep-lat/2202.12532].

[15] T. Doi and M.G. Endres, *Unified contraction algorithm for multi-baryon correlators on the lattice*, *Comput. Phys. Commun.* **184** (2013) 117 [hep-lat/1205.0585].

[16] HAL QCD collaboration, *Equation of State for Nucleonic Matter and its Quark Mass Dependence from the Nuclear Force in Lattice QCD*, *Phys. Rev. Lett.* **111** (2013) 112503 [hep-lat/1307.0299].

[17] HAL QCD collaboration, *Scale setting and hadronic properties in the light quark sector with (2+1)-flavor Wilson fermions at the physical point*, *Phys. Rev. D* **110** (2024) 094502 [hep-lat/2406.16665].

[18] http://bridge.kek.jp/Lattice-code/.

[19] S. Ueda, S. Aoki, T. Aoyama, K. Kanaya, H. Matsufuru, S. Motoki et al., *Development of an object oriented lattice QCD code 'Bridge++'*, *J. Phys. Conf. Ser.* **523** (2014) 012046.